

## RECONFIGURABLE COMPUTING AND NANOSCALE ARCHITECTURE

André DeHon

*Department of Electrical and Systems Engineering  
University of Pennsylvania*

For roughly four decades integrated circuits have been patterned top down with optical lithography, and feature sizes,  $F$ , have shrunk in a predictable, geometric fashion. With feature sizes now far below optical wavelengths (c.f. 400 nm violet light and 65 nm feature sizes) and approaching atomic lattice spacings (c.f. 65 nm feature sizes and 0.5 nm silicon lattice), it becomes more difficult and more expensive to pattern arbitrary features.

At the same time, fundamental advances in synthetic chemistry allow the assembly of structures made of a small and precise number of atoms, providing an alternate, bottom-up approach to constructing nanometer-scale devices. Rather than relying on ever-finer precision and control of lithography, bottom-up techniques exploit physical phenomena (e.g., molecular dimensions, film thicknesses composed of a precise number of atomic layers, nanoparticles constructed by self-limiting chemical processes) to directly define key feature sizes at the nanometer scale. Bottom-up fabrication gives us access to smaller feature sizes and promises more economical construction of atomic-scale devices and wires.

Both bottom-up structure synthesis and extreme subwavelength top-down lithography can produce small feature sizes only for very regular topologies. In optical lithography, regular interference patterns can produce regular structures with finer resolution than arbitrary topologies [1]. Bottom-up syntheses are limited to regular structures amenable to physical self-assembly.

Further, as noted in Chapter 37, construction at this scale, whether by top-down or bottom-up fabrication, exhibit high defect rates. High defect rates also drive increasing demand for regularity to support resource substitution.

At the same time, new technologies offer configurable switchpoints that can fit in the space of a nanoscale wire crossing (Section 38.2.3). The switches are much smaller than current SRAM configurable switches and can reduce the cost of reconfigurable architectures relative to ASICs. Smaller configurable switchpoints are particularly fortuitous because they make fine-grained configurability for defect tolerance viable.

High demand for regularity and fine-grained defect tolerance coupled with less expensive configurations increase the importance of reconfigurable architectures. Reconfigurable architectures can accommodate the requirements of

these atomic-scale technologies and exploit the density benefits they offer. Nonetheless, to fully accommodate and exploit these cost shifts, reconfigurable architectures continue to evolve.

This chapter reviews proposals for nanoscale configurable architectures that address the demands and opportunities of atomic-scale, bottom-up fabrication. It focuses on the nanoPLA architecture (see Section 38.6 and DeHon [2]), which has been specifically designed to exploit nanowires (Section 38.2.1) as the key building block. Despite the concrete focus on nanowires, many of the design solutions employed by the nanoPLA are applicable to other atomic-scale technologies. The chapter also briefly reviews nanoscale architectures (Section 38.7), which offer alternative solutions to key challenges in atomic-scale design.

---

## 38.1 TRENDS IN LITHOGRAPHIC SCALING

In the conventional, top-down lithographic model, we define a minimum, lithographically imageable feature size (i.e., half pitch,  $F$ ) and build devices that are multiples of this imageable feature size. Within the limits of this feature size, VLSI layout can perfectly specify the size of features and their location relative to each other in three dimensions—both in the two-dimensional plane of each lithographic layer and with adequate registration between layers. This gives complete flexibility in the layout of circuit structures as long as we adhere to the minimum imageable and repeatable feature size rules.

Two simplifying assumptions effectively made this possible: (1) Feature size was large compared to atoms, and (2) feature size was large compared to the wavelength of light used for imaging. With micron feature sizes, features were thousands of atoms wide and multiple optical wavelengths. As long as the two assumptions held, we did not need to worry about the discreteness of atoms nor the limits of optical lithography.

Today, however, we have long since passed the point where optical wavelengths are large compared to feature sizes, and we are rapidly approaching the point where feature sizes are measured in single-digit atom widths. We have made the transition to optical lithography below visible light (e.g., 193 nm wavelengths) and subwavelength imaging. Phase shift masking exploits interference of multiple light sources with different phases in order to define feature sizes finer than the wavelength of the source. This has allowed continued feature size scaling but increases the complexity and, hence, the cost of lithographic imaging.

Topology in the regions surrounding a pattern now impacts the fidelity of reproduction of the circuit or interconnect, creating the demand for optical proximity correction. As a result, we see an increase both in the complexity of lithographic mask generation and in the number of masks required. Region-based topology effects also limit the structures we can build. Because of both limitations in patterning and limitations in the analysis of region-based patterning effects, even in “full-custom” designs, we are driven to compose functions from a small palette of regular structures.

Rock's Law is a well-known rule of thumb in the semiconductor industry that suggests that semiconductor processing equipment costs increase geometrically as feature sizes shrink geometrically. One version of Rock's Law estimates that the cost of a semiconductor fabrication plant doubles every four years. Fabrication plants for the 90 nm generation were reported to cost \$2 to 3 billion.

The increasing cost comes from several sources, including the following:

- *Increasing demand for accuracy:* Alignment of features must scale with feature sizes.
- *Increasing demand for purity:* Smaller features mean that even smaller foreign particles (e.g., dust and debris) must be eliminated to prevent defects.
- *Increasing demand for device yield:* As noted in Chapter 37 (see Perfect yield, Section 37.2.3), to keep component yield constant, the per-device defect rate,  $P_d$ , must decrease as more devices are integrated onto each component.
- *Increasing processing steps:* More metal layers plus increasingly complex masks for optical resolution enhancement (described before) demand more equipment and processing.

It is already the case that few manufacturers can afford the capital investment required to develop and deploy the most advanced fabrication plants. Rising fabrication costs continue to raise the bar, forcing consolidation and centralization in integrated circuit manufacturing.

Starting at around 90 nm feature sizes, the mask cost per component typically exceeds \$1 million. This rising cost comes from the effects previously noted: more masks per component and greater complexity per mask. Coupled with rising component design and verification complexity, this raises the nonrecurring engineering (NRE) costs per chip design.

The economics of rising NRE ultimately lead to fewer unique designs. That is, if we hope to keep NRE costs to a small fraction—for example 10 percent—of the potential revenue for a chip, the market must be at least 10 times the NRE cost. With total NRE costs typically requiring tens of millions of dollars for 90 nm designs, each chip needs a revenue potential in the hundreds of millions of dollars to be viable. The bar continues to rise with NRE costs, decreasing the number of unique designs that the industry can support. This decrease in unique designs creates an increasing demand for differentiation after fabrication (i.e., reconfigurability).

---

## 38.2 BOTTOM-UP TECHNOLOGY

In contrast, bottom-up synthesis techniques give us a way to build devices and wires without relying on masks and lithography to define their atomic-scale features. They potentially provide an alternative path to device construction that may provide access to these atomic-scale features more economically than traditional lithography.

This section briefly reviews the bottom-up technology building blocks exploited by the nanoPLA, including nanowires (Section 38.2.1), ordered assembly of nanowires (Section 38.2.2), and programmable crosspoints (Section 38.2.3). These technologies are sufficient for constructing and understanding the basic nanoPLA design. For a roundup of additional nanoscale wire and crosspoint technologies, see the appendix in DeHon's 2005 article [2].

### 38.2.1 Nanowires

Chemists and material scientists are now regularly producing semiconducting and metallic wires that are nanometers in diameter and microns long using bottom-up synthesis techniques. To bootstrap the process and define the smallest dimensions, self-limiting chemical processes (e.g., Tan et al. [3]) can be used to produce nanoparticles of controlled diameter. From these nanoparticle seed catalysts, we can grow nanowires with diameters down to 3 nm [4]. The nanowire self-assembles into a crystalline lattice similar to planar silicon; however, growth is only enabled in the vicinity of the nanoparticle's catalyst. As a result, catalyst size defines the diameter of the grown nanowires [5]. Nanowires can be grown to millimeters in length [6], although it is more typical to work with nanowires tens of microns long [7].

Bottom-up synthesis techniques also allow the definition of atomic-scale features within a single nanowire. Using timed growth, features such as composition of different materials and different doping levels can be grown along the axis of the nanowire [8–10]. This effectively allows the placement of device features into nanowires, such as a field effect gateable region in the middle of an otherwise ungatetable wire (see Figure 38.1). Further, radial shells of different materials can be grown around nanowires with controlled thickness using timed growth [11, 12] or atomic-layer deposition [13, 14] (see Figure 38.2). These shells can be used to force the spacing between device and wire features, to act as dielectrics for field effect gating, or to build devices integrating heterogeneous materials with atomic-scale dimensions.

After a nanowire has been grown, it can be converted into a metal–silicon compound with lower resistance. For example, by coating select regions of

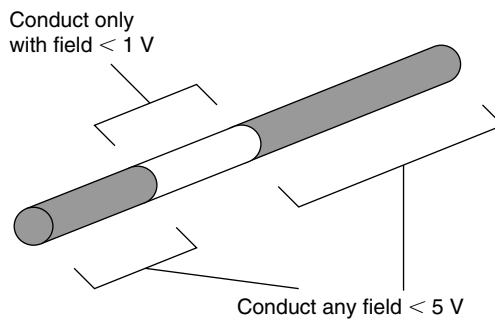


**FIGURE 38.1** ■ An axial doping profile. By varying doping along the axis of the nanowire, selectively gateable regions can be integrated into the nanowire.

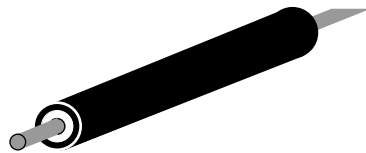


**FIGURE 38.2** ■ A radial doping profile.

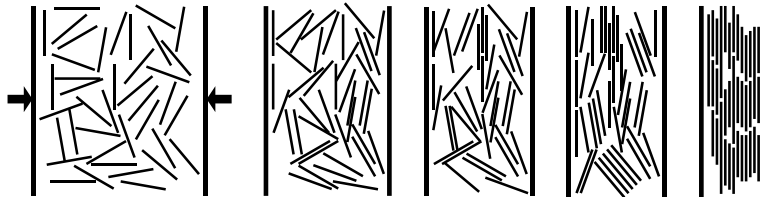


**FIGURE 38.3** ■ The Langmuir–Blodgett alignment of nanowires.

the nanowire with nickel and annealing, we can form a nickel–silicide (NiSi) nanowire [15]. The NiSi resistivity is much lower than the resistivity of heavily doped bulk silicon. Since nanowires have a very small cross-sectional area, this conversion is very important to keep the resistance, and hence the delay, of nanowires low. Further, this conversion is particularly important in reducing contact resistance between nanowires and lithographic-scale power supplies.

### 38.2.2 Nanowire Assembly

Langmuir–Blodgett (LB) flow techniques can be used to align a set of nanowires into a single orientation, close-pack them, and transfer them onto a surface [16, 17] (see Figure 38.3). The resulting wires are all parallel, but their ends may not be aligned. By using wires with an oxide sheath around the conducting core, the wires can be packed tightly without shorting together. The oxide sheath defines the spacing between conductors and can, optionally, be etched away after assembly. The LB step can be rotated and repeated so that we get multiple layers of nanowires [16, 18], such as crossed nanowires for building a wired-OR plane (Section 38.4.1).

### 38.2.3 Crosspoints

Many technologies have been demonstrated for nonvolatile, switched crosspoints. Common features include the following:

- Resistance that changes significantly between on and off states
- Ability to be made rectifying (i.e., to act as diodes)
- Ability to turn the device on or off by applying a voltage differential across the junction
- Ability to be placed within the area of a crossed nanowire junction

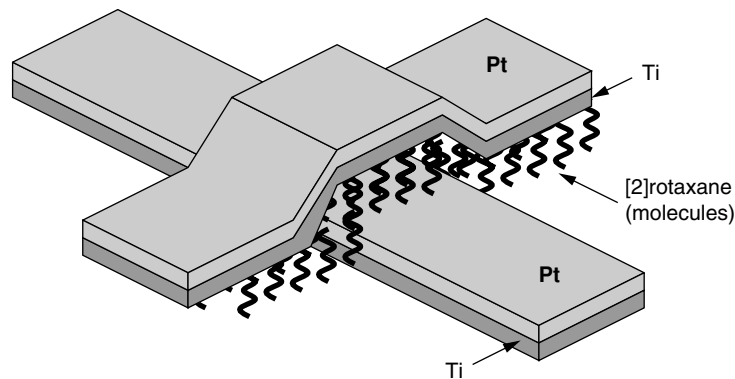


**FIGURE 38.4** ■ Switchable molecules sandwiched between nanoscale wires.

Chen et al. [19, 20] demonstrate a nanoscale Ti/Pt-[2]rotaxane-Ti/Pt sandwich (see Figure 38.4), which exhibits hysteresis and nonvolatile state storage showing an order of magnitude resistance difference between on and off states. The state of these devices can be switched at  $\pm 2\text{V}$  and read at  $\pm 0.2\text{V}$ . The basic hysteretic molecular memory effect is not unique to the [2]rotaxane, and the junction resistance is continuously tunable [21]. The exact nature of the physical phenomena involved is the subject of active investigation. LB techniques also can be used to place the switchable molecules between crossed nanowires (e.g., Collier et al. [22], Brown et al. [23]).

In conventional VLSI, the area of an SRAM-based programmable crosspoint switch is much larger than the area of a wire crossing. A typical CMOS switch might be  $600F^2$  [24], compared to a  $3F \times 3F$  bottom-level metal wire crossing, making the crosspoint more than 60 times the area of the wire crossing. Consequently, the nanoscale crosspoints offer an additional device size reduction beyond that implied by the smaller nanowire feature sizes. This particular device size benefit reduces the overhead for configurability associated with programmable architectures (e.g., FPGAs, PLAs) in this technology, compared to conventional CMOS.

### 38.3 CHALLENGES

Although the techniques reviewed in the previous section provide the ability to create very small feature sizes using the basic physical properties of materials to define dimensions, they also bring with them a number of challenges that any nanoscale architecture must address, including the following:

- *Required regularity in assembly and architecture:* These techniques do not allow the construction of arbitrary topologies; the assembly techniques limit us to regular arrays and crossbars of nanowires.

- *Lack of correlation in features:* The correlation between features is limited. It is possible to have correlated features within a nanowire, but only in a single nanowire; we cannot control which nanowire is placed next to which other nanowire or how they are aligned.
- *Differentiation:* If all the nanowires in a regular crossbar assembly behaved identically (e.g., were gated by the same inputs or were diode-connected to the same inputs), we would not get a benefit out of the nanoscale pitch. It is necessary to differentiate the function performed by the individual nanowires in order to exploit the benefits of their nanoscale pitch.
- *Signal restoration:* The diode crosspoints described in the previous section are typically nonrestoring; consequently, it is necessary to provide signal restoration for diode logic stages.
- *Defect tolerance:* We expect a high rate of defects in nanowires and crosspoints. Nanowires may break or make poor contacts. Crosspoints may have poor contact to the nanowires or contain too few molecules to be switched into a low-resistance state.

---

## 38.4 NANOWIRE CIRCUITS

It is possible to build a number of key circuits from the nanoscale building blocks introduced in the previous section, including a diode-based wired-OR logic array (Section 38.4.1) and a restoring nanoscale inverter (Section 38.4.2).

### 38.4.1 Wired-OR Diode Logic Array

The primary configurable structure we can build is a set of tight-pitched, crossed nanowires. With a programmable diode crosspoint at each nanowire intersection, this crossed nanowire array can serve as a programmable OR-plane. Assuming the diodes point from columns to rows (see Figure 38.5), each row output nanowire serves as a wired-OR for all of the inputs programmed into the low-resistance state. In the figure, programmed on crosspoints are shown in black; off crosspoints are shown in gray. Bold lines represent a nanowire pulled high, while gray lines remain low. Output nanowires are shown bold starting at the diode that pulls them high to illustrate current flow; the entire output nanowire would be pulled high in actual operation. Separate circuitry, not shown, is responsible for pulling wires low or precharging them low so that an output remains low when no inputs can pull it high.

Consider a single-row nanowire, and assume for the moment that there is a way to pull a nondriven nanowire down to ground. If any of the column nanowires that cross this row nanowire are connected with low-resistance crosspoint junctions and are driven to a high voltage level, the current into the column nanowire will be able to flow into the row nanowire and charge it up to a higher voltage value (see O1, O3, O4, and O5 in Figure 38.5). However, if none of

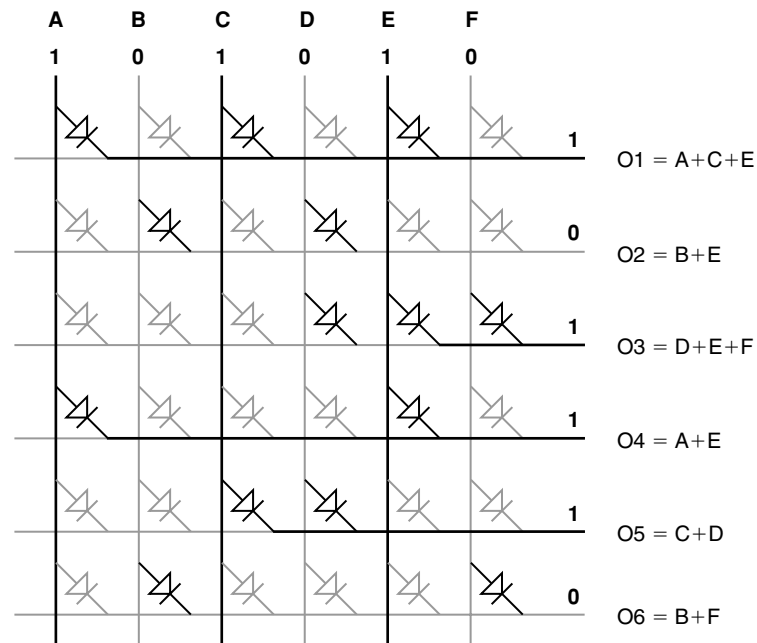


**FIGURE 38.5** ■ The wired-OR plane operation.

the connected column nanowires is high, the row nanowire will remain low (see O2 and O6 in the figure). Consequently, the row nanowire effectively computes the OR of its programmed inputs.

The output nanowires do pull their current directly off the inputs and may not be driven as high as the input voltage. Consequently, these outputs will require restoration (Section 38.4.2).

A special use of the wired-OR programmable array is for interconnect. That is, if we restrict ourselves to connecting a *single* row wire to each column wire, the crosspoint array can serve as a crossbar switch. This allows any input (column) to be routed to any output (row) (see Figure 38.6). This structure is useful for postfabrication programmable routing to connect logic functions and to avoid defective resources. In the figure, programmed on crosspoints are shown in black; off crosspoints are shown in gray. This means that the crossbar shown in the figure is programmed to connect  $A \rightarrow T$ ,  $B \rightarrow Q$ ,  $C \rightarrow V$ ,  $D \rightarrow S$ ,  $E \rightarrow U$ , and  $F \rightarrow R$ .

### 38.4.2 Restoration

As noted in Section 38.4.1, the programmable, wired-OR logic is passive and nonrestoring, drawing current from the input. Further, OR logic is not universal. To build a good, composable logic family, we need to be able to isolate inputs from output loads, restore signal strength and current drive, and invert signals.



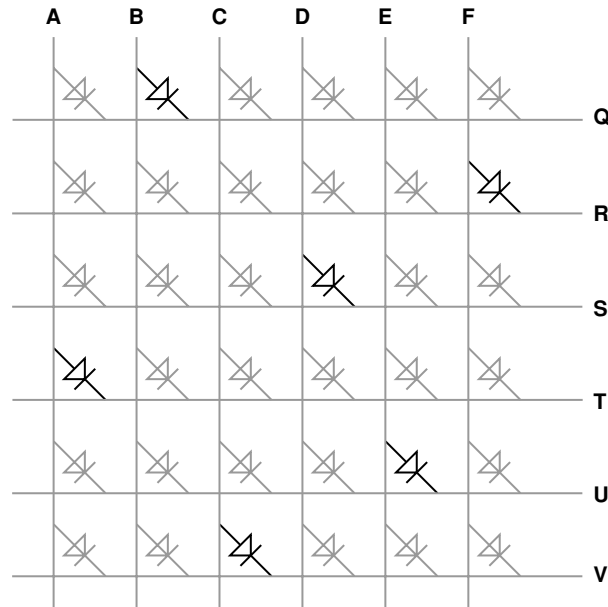


**FIGURE 38.6** ■ An example crossbar routing configuration.

Fortunately, nanowires can be field effect controlled. This provides the potential to build gates that behave like field effect transistors (FETs) for restoration. However, to realize them, we must find ways to create the appropriate gate topology within regular assembly constraints (Section 38.5).

If two nanowires are separated by an insulator, perhaps using an oxide core shell, we can use the field from one nanowire to control the other nanowire. Figure 38.7 shows an inverter built using this basic idea. The horizontal nanowire serves as the input and the vertical nanowire as the output. This gives a voltage transfer equation of

$$V_{out} = V_{high} \left( \frac{R_{pd}}{R_{pd} + R_{fet}(\text{Input}) + R_{pu}} \right) \quad (38.1)$$

For the sake of illustration, the vertical nanowire has a lightly doped P-type depletion-mode region at the input crossing that forms a FET controlled by the input voltage ( $R_{fet}(\text{Input})$ ). Consequently, a low voltage on the input nanowire allows conduction through the vertical nanowire ( $R_{fet} = R_{on-fet}$  is small), and a high input depletes the carriers from the vertical nanowire and prevents conduction ( $R_{fet} = R_{off-fet}$  is large). As a result, a low input allows the nanowire to conduct and pull the output region of the vertical nanowire up to a high voltage. A high input prevents conduction and the output region remains low. A second crossed region on the nanowire is used for the pulldown ( $R_{pd}$ ). This region can be used as a gate for predischarging the output so that the inverter is pulled low

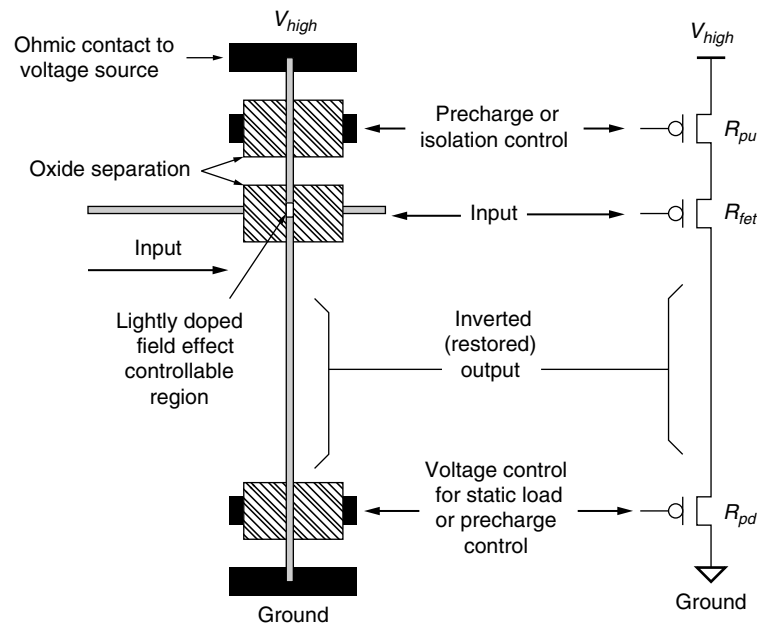


FIGURE 38.7 ■ A nanowire inverter.

before the input is applied, then left high to disconnect the pulldown voltage during evaluation. Alternatively, it can be used as a static load for PMOS-like ratioed logic. By swapping the location of the high- and low-power supplies, this same arrangement can be used to buffer rather than invert the input.

Note that the gate only loads the input capacitively. Consequently, the output current is isolated from the input current at this inverter or buffer. Further, nanowire field effect gating has sufficient nonlinearity so that this gate provides gain to restore logic signal levels [25].

## 38.5 STATISTICAL ASSEMBLY

One challenge posed by regular structures, such as tight-pitch nanowire cross-bars, is differentiation. If all the wires are the same and are fabricated at a pitch smaller than we can build arbitrary topologies lithographically, how can we selectively address a single nanowire? If we had enough control to produce arbitrary patterns at the nanometer scale, we could build a decoder (see Figure 38.8) to provide pitch-matching between this scale and the scale at which we could define arbitrary topologies.

The trick is to build the decoder statistically. That is, differentiate the nanowires by giving each one an address, randomly select the nanowires that go into each array, and carefully engineer the statistics to guarantee a high

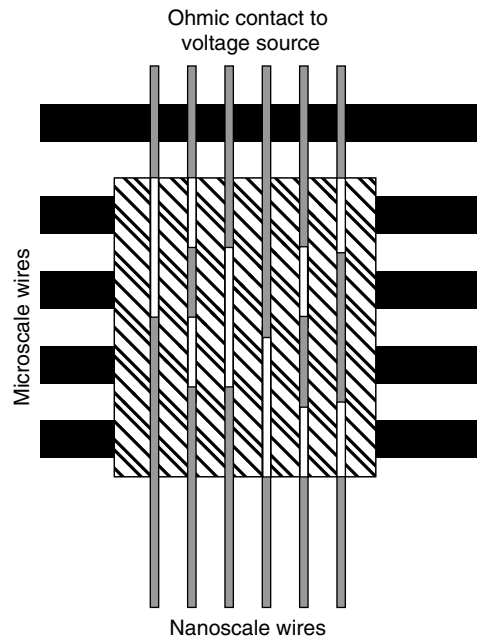


**FIGURE 38.8** ■ A decoder for addressing individual nanowires assembled at nanoscale pitch.

probability that there will be a unique address associated with each nanowire in each nanowire array. We can use axial doping to integrate the address into each nanowire [26].

If we pick the address space sparsely enough, Law of Large Numbers statistics can guarantee unique addressability of the nanowires. For example, if we select 10 nanowires out of a large pool with  $10^6$  different nanowire types, we get a unique set of nanowires more than 99.99 percent of the time. In general, we can guarantee more than 99 percent probability of uniqueness of  $N$  nanowires using only  $100N^2$  addresses [26]. By allowing a few duplications, the address space can be much smaller [27].

Statistical selection of coded nanowires can also be used to assemble nanoscale wires for restoration [2]. As shown in Figure 38.9(a), if coded nanowires can be perfectly placed in an array, we can build the restoration circuit shown in Section 38.4.2 (Figure 38.7) and arrange them to restore the outputs of a wired-OR array. However, the bottom-up techniques that can assemble these tight-pitch feature sizes cannot order or place individual nanowires and cannot provide correlation between nanowires. As shown in Figure 38.9(b), statistical alignment and placement of the restoration nanowires can be used to construct the restoration array. Here, not every input will be restored, but the Law of Large Numbers guarantees that we can restore a reliably predictable fraction of the inputs. For further details, see DeHon [2, 27].

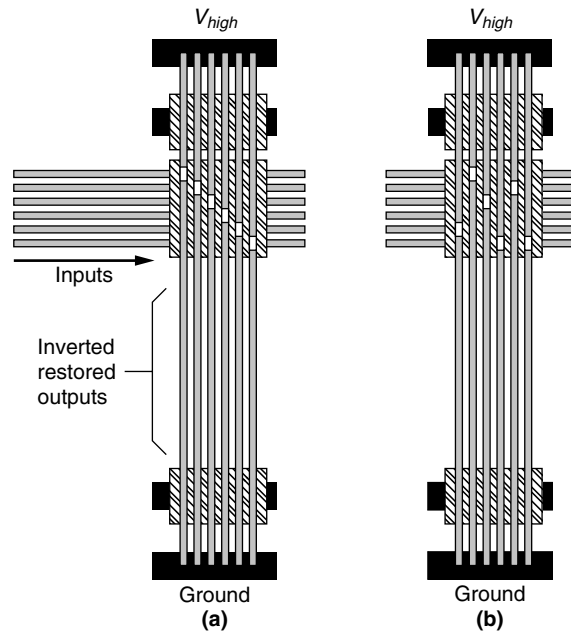


**FIGURE 38.9** ■ A restoration array: (a) ideal and (b) stochastic.

## 38.6 NANOPLA ARCHITECTURE

With these building blocks we can assemble a complete reconfigurable architecture. This section starts by describing the PLA-based logic block (Section 38.6.1), then shows how PLAs are connected together into an array of interconnected logic blocks (Section 38.6.2). It also notes that nanoscale memories can be integrated with this array (Section 38.6.3), reviews the defect tolerance approach for this architecture (Section 38.6.4), describes how designs are mapped to nanoPLA designs (Section 38.6.5), and highlights the density benefits offered by the technology (Section 38.6.6).

### 38.6.1 Basic Logic Block

The nanoPLA architecture combines the wired-OR plane, the stochastically assembled restoration array, and the stochastic address decoder to build a simple, regular PLA array (see Figure 38.10). The stochastic decoder described in Section 38.5 allows individual nanowires to be addressed from the lithographic scale for testing and programming (see Figures 38.11 and 38.12). The output of the programmable, wired-OR plane is restored via a restoration plane using field effect gating of the crossed nanowire set as described in Section 38.5 and shown in Figure 38.9.

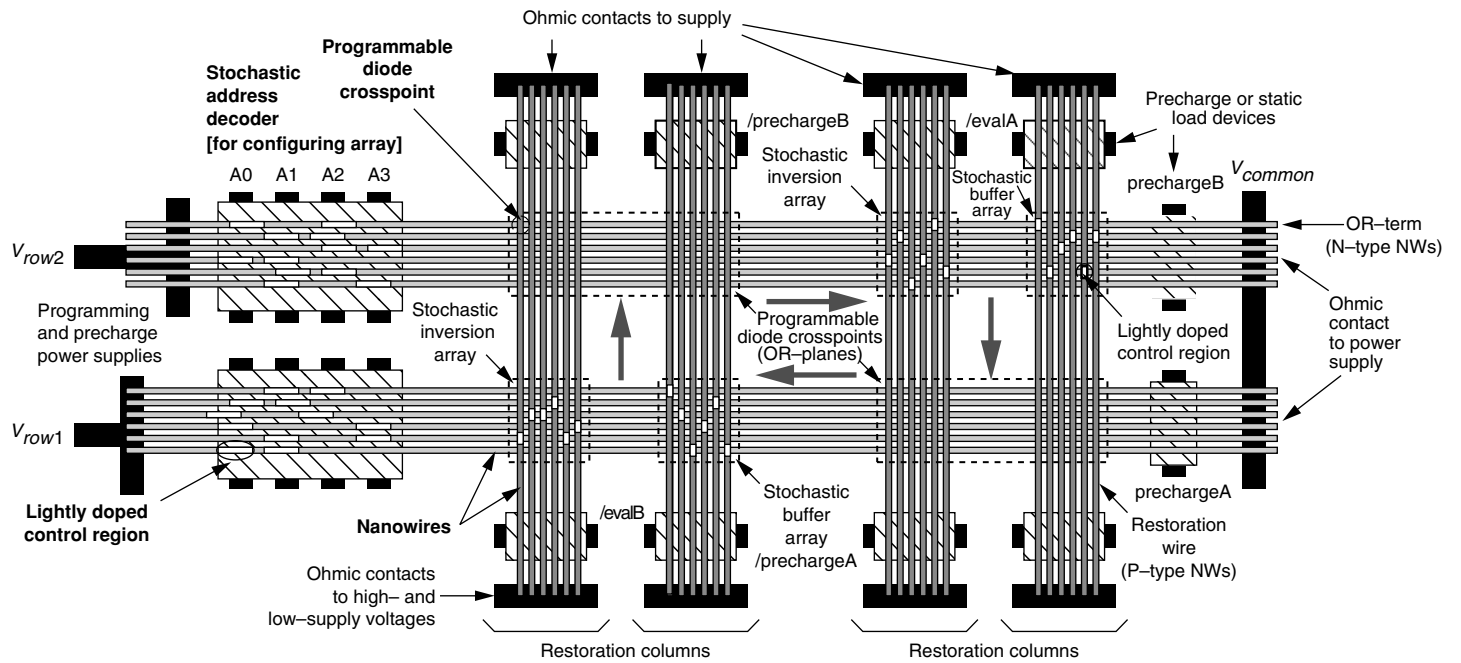


FIGURE 38.10 ■ A simple nanoPLA block.

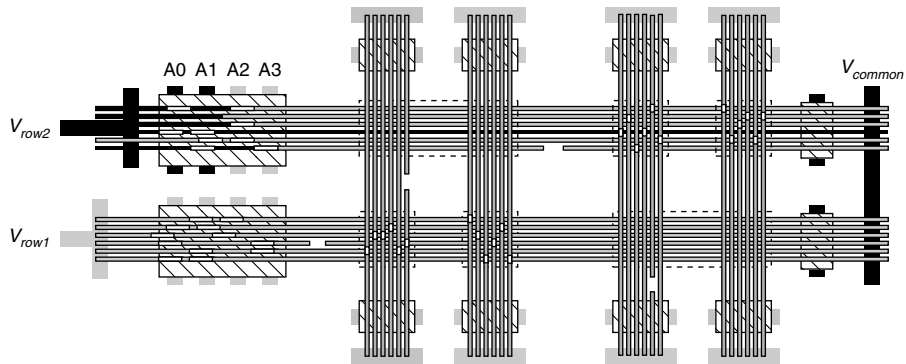


FIGURE 38.11 ■ Addressing a single nanowire.

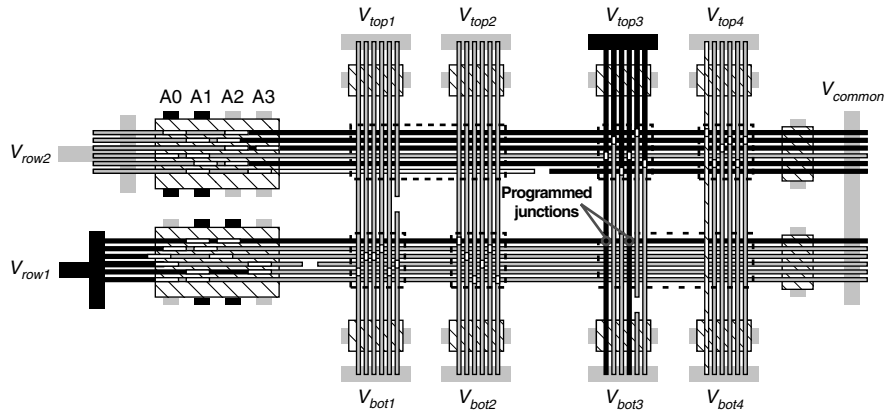


FIGURE 38.12 ■ Programming a nanowire–nanowire crosspoint.

As shown in Figure 38.11, an address is applied on the lithographic-scale address lines (A0 ... A3). The applied address (1100) allows conduction through only a single nanowire. By monitoring the voltage at the common lithographic node at the far end of the nanowire ( $V_{common}$ ), it is possible to determine whether the address is present and whether the wire is functional (e.g., not broken). By monitoring the timing of the signal on  $V_{common}$ , we may be able to determine the resistance of the nanowire.

As shown in Figure 38.12, addresses are applied to the lithographic-scale address lines of both the top and bottom planes to select individual nanowires in each plane. We use the stochastic restoration columns to turn the corner between the top plane and the restoration inputs to the bottom plane. Note that since column 3 is an inverting column, we arrange for the single, selected signal on the top plane to be a low value. Since the stochastic assembly resulted in two

restoration wires for this input, both nanowire inputs are activated. As a result, we place the designated voltage across the two marked crosspoints to turn on the crosspoint junctions between the restored inputs and the selected nanowire in the bottom plane.

The restoration planes can provide inversion such that the pair of planes serve as a programmable NOR. The two back-to-back NOR planes can be viewed as a traditional AND-OR PLA with suitable application of DeMorgan's Law. A second set of restoration wires provides buffered, noninverted inputs to the next wired-OR plane; in this manner, each plane gets the true and complement version of each logical signal just as is normally provided at the inputs to a VLSI PLA. Microscale field effect gates (e.g., /evalA and /evalB) control when nanowire logic can evaluate, allowing the use of a familiar 2-phase clocking discipline. As such, the PLA cycle shown in Figure 38.10 can directly implement an FSM. Programmable crosspoints can be used to personalize the array, avoid defective wires and crosspoints (Section 38.6.4), and implement a deterministic function despite fabrication defects and stochastic assembly.

### 38.6.2 Interconnect Architecture

To construct larger components using the previously described structures, we can build an array of nanoPLA blocks, where each block drives outputs that cross the input (wired) regions of many other blocks (Figure 38.13) [2, 28]. This allows the construction of modest-size PLAs (e.g., 100 Pterms), which are efficient for logic mapping and keep the nanowire runs short (e.g., 10  $\mu\text{m}$ ) in order to increase yield and avoid the high resistance of long nanowires. The nanoPLA blocks provide logic units, signal switching, and signal buffering for long wire runs. With an appropriate overlap topology, such nanoPLAs can support Manhattan (orthogonal X-Y) routing similar to conventional, island-style FPGA architectures (Chapter 1).

By stacking additional layers of nanowires, the structure can be extended vertically into the third dimension [29]. Programmable and gateable junctions between adjacent nanowire layers allow routing up and down the nanowire stack. This provides a path to continue scaling logic density when nanowire diameters can shrink no further.

The resulting nanoPLA structure is simple and very regular. Its high-density features are built entirely from tight-pitched nanowire arrays. All the nanowire array features are defined using bottom-up techniques. The overlap topology between nanowires is carefully arranged so that the output of a function (e.g., wired-OR, restoration, routing) is a segment of a nanowire that then crosses the active or input portion of another function. Regions (e.g., wired-OR, restoration) are differentiated at a lithographic scale. Small-scale differentiation features are built into the nanowires and statistically populated (e.g., addressing, restoration).

In the nanoPLA, the wired-OR planes combine the roles of switchbox, connection box, and logic block into one unified logic and switching plane. The wired-OR plane naturally provides the logic block in a nanoPLA block. It also serves

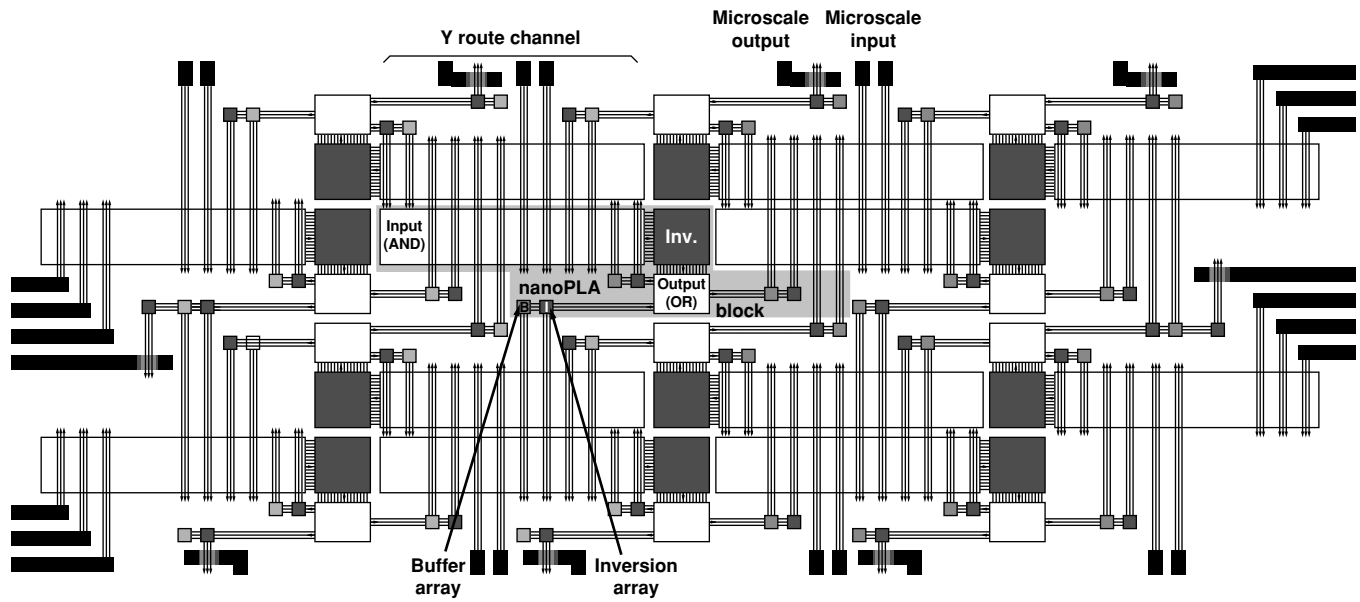


**FIGURE 38.13** ■ nanoPLA block tiling with edge I/O to lithographic scale.



to select inputs from the routing channel that participate in the logic. Signals that must be rebuffed or switched through a block are also routed through the same wired-OR plane. Since the configurable switchpoints fit within the space of a nanowire crossing, the wired-OR plane (hence the interconnect switching) can be fully populated unlike traditional FPGA switch blocks that have a very limited population to reduce their area requirements.

### 38.6.3 Memories

The same basic crosspoints and nanowire crossbar used for the wired-OR plane (Section 38.4.1) can also serve as the core of a memory bank. An address decoder similar to the one used for programming the wired-OR array (see Section 38.5 and Figure 38.8) supports read/write operations on the memory core [26, 30]. Unique, random addresses can be used to configure deterministic memory addresses, avoiding defective memory rows and columns [31]. A full-component architecture would interleave these memory blocks with the nanoPLA logic blocks similar to the way memory blocks are embedded in conventional FPGAs (Chapter 1).

### 38.6.4 Defect Tolerance

Nanowires in each wired-OR plane and interconnect channel are locally substitutable (see the Local sparing subsection in Section 37.2.4). The full population of the wired-OR crossbar planes guarantees this is true even for the interconnect channels. We provision spare nanowires based on their defect rate, as suggested in the Yield with sparing subsection of Section 37.2.3. For each array, we test for functional wires as illustrated in Section 38.6.1. Logical Pterms are assigned to nanowires using the matching approach described in the Fine-grained Pterm matching subsection of Section 37.2.5. For a detailed description of nanoPLA defect tolerance, see DeHon and Naeimi [32].

### 38.6.5 Design Mapping

Logic-level designs can be mapped to the nanoPLA. The logic and physical mapping for the nanoPLA uses similar techniques to those introduced in Part III. Starting from a logic netlist, technology mapping can be performed using PLAmapping (see Section 13.3.4) to generate two-level clusters for each nanoPLA block, which can then be placed using an annealing-based placer (Chapter 14). Routing is performed with a PathFinder-based router (Chapter 17). Because of the full population of the switchboxes, the nanoPLA router need only perform global routing. Since nanoPLA blocks provide both logic and routing, the router must also account for the logic assigned to each nanoPLA block when determining congestion. As noted before, at design loadtime, logical Pterms are assigned to specific nanowires using a greedy matching approach (see the Fine-grained Pterm matching subsection of Section 37.2.5).

### 38.6.6 Density Benefits

Despite statistical assembly, lithographic overheads for nanowire addressing, and high defect rates, small feature sizes, and compact crosspoints can offer a significant density advantage compared to lithographic FPGAs. When mapping the Toronto 20 benchmark suite [33] to 10-nm full-pitch nanowires (e.g., 5-nm-diameter nanowires with 5-nm spacing between nanowires), we typically see two orders of magnitude greater density than with defect-free 22-nm lithographic FPGAs [2]. As noted earlier, areal density can be further increased by using additional layers of nanowires [29].

## 38.7 NANOSCALE DESIGN ALTERNATIVES

Several architectures have been proposed for nanoscale logic. A large number are also based on regular crossbar arrays and look similar to the nanoPLA at a gross level (see Table 38.1). Like the nanoPLA, all these schemes employ fine-grained configurability to tolerate defects. Within these architectures there are different ways to address the key challenges (Section 38.3). These architectures enrich the palette of available component solutions, increasing the likelihood of assembling a complementary set of technology and design elements to practically realize nanoscale configurable logic.

### 38.7.1 Imprint Lithography

In the concrete technology described in Section 38.2, seeded nanowire growth was used to obtain small feature sizes and LB flow to assemble them into parallel arrays. Another emerging technique for producing regular, nanoscale structures (e.g., a set of parallel, tight-pitched wires) is imprint lithography. The masks for imprint lithography can be generated using bottom-up techniques.

**TABLE 38.1** ■ A comparison of nano-electronic programmable logic designs

Component element	HP/UCLA crossbar architecture	CMU nanoFabric	nanoPLA	Stony Brook CMOL	Hewlett-Packard FPNI
Crosspoint technology	Programmable diode	Programmable diode	Programmable diode	Programmable diode	Programmable diode
Nanowire technology	Nano-imprint lithography	Nanopore templates	Catalyst nanowires	Nano-imprint lithography	Nano-imprint lithography
Logic implementation	Nanoscale wired-OR	Nanoscale wired-OR	Nanoscale wired-OR	Nanoscale wired-OR	Lithoscale (N)AND2
CMOS↔Nanowire interface	Random particles	—	Coded nanowires	Crossbar tilt	Crossbar tilt
Restoration	CMOS	RTD latch	nanowire FET	CMOS	CMOS
References	[34, 35, 36]	[37, 38]	[28, 39]	[40]	[41]

In one scheme, timed vertical growth or atomic-layer deposition on planar semiconductors is used to define nanometer-scale layers of differentially etchable materials. Cut orthogonally, the vertical cross-section can be etched to produce a comblike structure where the teeth, as well as the spacing between them, are single-digit nanometers wide (e.g., 8 nm). The resulting structure can serve as a pattern for nanoscale imprint lithography [42, 43] to produce a set of tight-pitched, parallel lines. That is, the long parallel lines resulting from the differential etch can be stamped into a resist mask [43], which is then etched to produce a pattern in a polymer or coated with metal to directly transfer metallic lines to a substrate [42]. These techniques can produce regular nanostructures but cannot produce arbitrary topologies.

### 38.7.2 Interfacing

When nanowires are fabricated together using imprint lithography, it is not possible to uniquely construct and code nanowires as exploited for addressing in the nanoPLA (Section 38.5). Williams and Kuekes [36] propose the first randomized decoder scheme for differentiating nanoscale wires and interfacing between lithographic and nanoscale feature sizes. They use a physical process to randomly deposit metal particles between the lithographic-scale address lines and the nanoscale wires. A nanowire is controllable by an address wire only if it has a metal particle bridging it to the address line. Unlike the nanowire-coding scheme where addresses are selected from a carefully chosen address space and grown into each nanowire (Section 38.5), in this scheme the address on each nanowire is randomly generated. As a result, this scheme requires 2 to 2.5 times as many address wires as the statistically assembled nanowire-coding scheme.

Alternately, Strukov and Likharev [40, 44] observe that it should be possible to directly connect each long crossbar nanowire by a nanovia to lithographic-scale circuitry that exists below the nanoscale circuits. The *nanovia* is a semiconductor pin spaced at lithographic distances and grown with a taper to a nanoscale tip for interfacing with individual nanowires. An array of these pins (e.g., Jensen [45]) can provide nanovia interfaces.

The key idea is to pitch-match the lithographically spaced nanovia pins with the nanoscale pitch nanowires and guarantee that there is space in the CMOS below the nanoscale circuitry for the CMOS restoration and programming circuits. Note of the following:

- Nanoscale wires can be angled relative to the CMOS circuitry to match the pitch of the CMOS nanovias to the nanoscale wires. Figure 38.14 shows this tilt interfacing to a single nanowire array layer. Nanovias that connect to the CMOS are arranged in a square array with side  $2\beta F_{CMOS}$ , where  $F_{CMOS}$  is the half-pitch of the CMOS subsystem, and  $\beta$  is a dimensionless factor larger than 1 that depends on CMOS cell complexity. The nanowire crossbar is turned by an angle  $\alpha = \arcsin(F_{nano}/\beta F_{CMOS})$  relative to the CMOS pin array, where  $F_{nano}$  is the nanowire half-pitch.

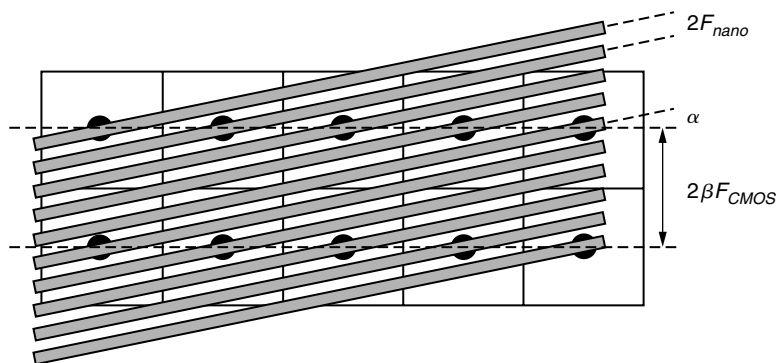


**FIGURE 38.14** ■ Nanoscale and CMOS pitch matching via tilt.

- If sufficiently long nanowires are used, the area per nanowire can be as large as each CMOS cell (e.g., restoration buffer and programming transistors). For example, if we use  $10\mu\text{m}$  nanowires at  $10\text{ nm}$  pitch, each nanowire occupies  $10^5\text{ nm}^2$ ; each such nanowire could have its own  $300\text{ nm} \times 300\text{ nm}$  CMOS cell ( $\beta \approx 3$  for  $F_{\text{CMOS}} = 45\text{ nm}$ ) and keep the CMOS area contained below the nanowire area.

For detailed development of this interface scheme, see Likharev and Strukov [44]. Hewlett-Packard employs a variant of the tilt scheme for their field-programmable nanowire interconnect (FPNI) architecture [41].

### 38.7.3 Restoration

Enabled by the array-tilt scheme that allows each nanowire to be directly connected to CMOS circuitry, the hybrid semiconductor-molecular electronics (CMOL) and FPNI nanoscale array designs use lithographic-scale CMOS buffers to perform signal restoration and inversion. CMOS buffers with large feature sizes will be larger than nanowire FETs and have less variation. The FPNI scheme uses nanoscale configurability only to provide programmable interconnect, using a nonconfigurable 2-input CMOS NAND/AND gate for logic.

Alternatively, it may be possible to build latches that provide gain and isolation from 2-terminal molecular devices [38]. Specifically, molecules that serve as resonant-tunneling diodes (RTDs) or negative differential resistors have been synthesized [46, 47]. These devices are characterized by a region of negative resistance in their IV-curve. The CMU nanoFabric design shows how to build and integrate latches based on RTD devices. The latches draw their power from the clock and provide restoration and isolation.

## 38.8 SUMMARY

Between highly regular structures and high defect rates, atomic-scale design appears to demand postfabrication configurability. This chapter shows how

configurable architectures can accommodate the extreme regularity required. It further shows that configurable architectures can tolerate extremely limited control during the fabrication process by exploiting large-scale assembly statistics. Consequently, we obtain a path to denser logic using building blocks roughly 10 atoms wide, as well as a path to continued integration in the third dimension.

Spatially configurable design styles become even more important when all substrates are configurable at their base level. We can always configure sequential processors on top of these nanoscale substrates when tasks are irregular and low throughput (see Chapter 36 and the Processor subsection of Section 5.2.2). However, when tasks can be factored into regular subtasks, direct spatial implementation on the configurable substrate will be more efficient, reducing both runtime and energy consumption.

## References

- [1] S. R. J. Brueck. There are no fundamental limits to optical lithography. *International Trends in Applied Optics*, SPIE Press, 2002.
- [2] A. DeHon. Nanowire-based programmable architectures. *ACM Journal on Emerging Technologies in Computing Systems* 1(2), 2005.
- [3] Y. Tan, X. Dai, Y. Li, D. Zhu. Preparation of gold, platinum, palladium and silver nanoparticles by the reduction of their salts with a weak reductant—potassium bitartrate. *Journal of Material Chemistry* 13, 2003.
- [4] Y. Wu, Y. Cui, L. Huynh, C. J. Barrelet, D. C. Bell, C. M. Lieber. Controlled growth and structures of molecular-scale silicon nanowires. *Nanoletters* 4(3), 2004.
- [5] Y. Cui, L. J. Lauhon, M. S. Gudiksen, J. Wang, C. M. Lieber. Diameter-controlled synthesis of single crystal silicon nanowires. *Applied Physics Letters* 78(15), 2001.
- [6] B. Zheng, Y. Wu, P. Yang, J. Liu. Synthesis of ultra-long and highly-oriented silicon oxide nanowires from alloy liquid. *Advanced Materials* 14, 2002.
- [7] M. S. Gudiksen, J. Wang, C. M. Lieber. Synthetic control of the diameter and length of semiconductor nanowires. *Journal of Physical Chemistry B* 105, 2001.
- [8] M. S. Gudiksen, L. J. Lauhon, J. Wang, D. C. Smith, C. M. Lieber. Growth of nanowire superlattice structures for nanoscale photonics and electronics. *Nature* 415, 2002.
- [9] Y. Wu, R. Fan, P. Yang. Block-by-block growth of single-crystalline Si/SiGe superlattice nanowires. *Nanoletters* 2(2), 2002.
- [10] M. T. Björk, B. J. Ohlsson, T. Sass, A. I. Persson, C. Thelander, M. H. Magnusson, K. Depper, L. R. Wallenberg, L. Samuelson. One-dimensional steepelchase for electrons realized. *Nanoletters* 2(2), 2002.
- [11] L. J. Lauhon, M. S. Gudiksen, D. Wang, C. M. Lieber. Epitaxial core-shell and core-multi-shell nanowire heterostructures. *Nature* 420, 2002.
- [12] M. Law, J. Goldberger, P. Yang., Semiconductor nanowires and nanotubes. *Annual Review of Material Science* 34, 2004.
- [13] M. Ritala. Advanced ALE processes of amorphous and polycrystalline films. *Applied Surface Science* 112, 1997.
- [14] M. Ritala, K. Kukli, A. Rahtu, P. I. Räisänen, M. Leskelä, T. Sajavaara, J. Keinonen. Atomic layer deposition of oxide thin films with metal alkoxides as oxygen sources. *Science* 288, 2000.

- [15] Y. Wu, J. Xiang, C. Yang, W. Lu, C. M. Lieber. Single-crystal metallic nanowires and metal/semiconductor nanowire heterostructures. *Nature* 430, 2004.
- [16] Y. Huang, X. Duan, Q. Wei, C. M. Lieber. Directed assembly of one-dimensional nanostructures into functional networks. *Science* 291, 2001.
- [17] D. Whang, S. Jin, C. M. Lieber. Nanolithography using hierarchically assembled nanowire masks. *Nanoletters* 3(7), 2003.
- [18] D. Whang, S. Jin, Y. Wu, C. M. Lieber. Large-scale hierarchical organization of nanowire arrays for integrated nanosystems. *Nanoletters* 3(9), 2003.
- [19] Y. Chen, D. A. A. Ohlberg, X. Li, D. R. Stewart, R. S. Williams, J. O. Jeppesen, K. A. Nielsen, J. F. Stoddart, D. L. Olynick, E. Anderson. Nanoscale molecular-switch devices fabricated by imprint lithography. *Applied Physics Letters* 82(10), 2003.
- [20] Y. Chen, G.-Y. Jung, D. A. A. Ohlberg, X. Li, D. R. Stewart, J. O. Jeppesen, K. A. Nielsen, J. F. Stoddart, R. S. Williams. Nanoscale molecular-switch crossbar circuits. *Nanotechnology* 14, 2003.
- [21] D. R. Stewart, D. A. A. Ohlberg, P. A. Beck, Y. Chen, R. S. Williams, J. O. Jeppesen, K. A. Nielsen, J. F. Stoddart. Molecule-independent electrical switching in Pt/organic monolayer/Ti devices. *Nanoletters* 4(1), 2004.
- [22] C. Collier, G. Mattersteig, E. Wong, Y. Luo, K. Beverly, J. Sampaio, F. Raymo, J. Stoddart, J. Heath. A [2]catenane-based solid state reconfigurable switch. *Science* 289, 2000.
- [23] C. L. Brown, U. Jonas, J. A. Preece, H. Ringsdorf, M. Seitz, J. F. Stoddart. Introduction of [2]catenanes into Langmuir films and Langmuir-Blodgett multilayers: A possible strategy for molecular information storage materials. *Langmuir* 16(4), 2000.
- [24] A. DeHon. Reconfigurable Architectures for General-Purpose Computing. AI Technical Report 1586, MIT Artificial Intelligence Laboratory, Cambridge, MA, 1996.
- [25] A. DeHon. Array-based architecture for FET-based, nanoscale electronics. *IEEE Transactions on Nanotechnology* 2(1), 2003.
- [26] A. DeHon, P. Lincoln, J. Savage. Stochastic assembly of sublithographic nanoscale interfaces. *IEEE Transactions on Nanotechnology* 2(3), 2003.
- [27] A. DeHon. Law of Large Numbers system design. In *Nano, Quantum and Molecular Computing: Implications to High Level Design and Validation*, Kluwer Academic, 2004.
- [28] A. DeHon. Design of programmable interconnect for sublithographic programmable logic arrays. *Proceedings of the International Symposium on Field-Programmable Gate Arrays*, 2005.
- [29] B. Gojman, R. Rubin, C. Pilotto, T. Tanamoto, A. DeHon. 3D nanowire-based programmable logic. *Proceedings of the International Conference on Nano-Networks* 2006.
- [30] A. DeHon, S. C. Goldstein, P. J. Kuekes, P. Lincoln. Non-photolithographic nanoscale memory density prospects. *IEEE Transactions on Nanotechnology* 4(2), 2005.
- [31] A. DeHon. Deterministic addressing of nanoscale devices assembled at sublithographic pitches. *IEEE Transactions on Nanotechnology* 4(6), 2005.
- [32] A. DeHon, H. Naeimi. Seven strategies for tolerating highly defective fabrication. *IEEE Design and Test of Computers* 22(4), 2005.
- [33] V. Betz, J. Rose. FPGA Place-and-Route Challenge. <http://www.eecg.toronto.edu/~vaughn/challenge/challenge.html>, 1999.

- [34] J. R. Heath, P. J. Kuekes, G. S. Snider, R. S. Williams. A defect-tolerant computer architecture: Opportunities for nanotechnology. *Science* 280(5370), 1998.
- [35] Y. Luo, P. Collier, J. O. Jeppesen, K. A. Nielsen, E. Delonno, G. Ho, J. Perkins, H.-R. Tseng, T. Yamamoto, J. F. Stoddart, J. R. Heath. Two-dimensional molecular electronics circuits. *ChemPhysChem* 3(6), 2002.
- [36] S. Williams, P. Kuekes. Demultiplexer for a molecular wire crossbar network. U.S. Patent number 6,256,767, July 3, 2001.
- [37] S. C. Goldstein, M. Budiu. NanoFabrics: Spatial computing using molecular electronics. *Proceedings of the International Symposium on Computer Architecture* 178–189, 2001.
- [38] S. C. Goldstein, D. Rosewater. Digital logic using molecular electronics. *ISSCC Digest of Technical Papers*, IEEE, 2002.
- [39] A. DeHon, M. J. Wilson. Nanowire-based sublithographic programmable logic arrays. *Proceedings of the International Symposium on Field-Programmable Gate Arrays*, 2004.
- [40] D. B. Strukov, K. K. Likharev. CMOL FPGA: A reconfigurable architecture for hybrid digital circuits with two-terminal nanodevices. *Nanotechnology* 16(6), 2005.
- [41] G. S. Snider, R. S. Williams. Nano/CMOS architectures using a field-programmable nanowire interconnect. *Nanotechnology* 18(3), 2007.
- [42] N. A. Melosh, A. Boukai, F. Diana, B. Gerardot, A. Badolato, P. M. Petroff, J. R. Heath. Ultra high-density nanowire lattices and circuits. *Science* 300, 2003.
- [43] M. D. Austin, H. Ge, W. Wu, M. Li, Z. Yu, D. Wasserman, S. A. Lyon, S. Y. Chou. Fabrication of 5 nm linewidth and 14 nm pitch features by nanoimprint lithography. *Applied Physics Letters* 84(26), 2004.
- [44] K. K. Likharev, D. B. Strukov. CMOL: Devices, circuits, and architectures. In *Introducing Molecular Electronics*, Springer, 2005.
- [45] K. L. Jensen. Field emitter arrays for plasma and microwave source applications. *Physics of Plasmas* 6(5), 1999.
- [46] J. Chen, M. Reed, A. Rawlett, J. Tour. Large on-off ratios and negative differential resistance in a molecular electronic device. *Science* 286, 1999.
- [47] J. Chen, W. Wang, M. A. Reed, M. Rawlett, D. W. Price, J. M. Tour. Room-temperature negative differential resistance in nanoscale molecular junctions. *Applied Physics Letters* 77, 2000.